

RESEARCH ARTICLE

Fuzzy inference system model for the spectrum site coefficients of the Türkiye Building Earthquake Code (2018)

Vefa Okumuş¹, Atakan Mangır¹

¹ Istanbul Medipol University, Department of Civil Engineering, Istanbul, Türkiye

Article History

Received 23 May 2023 Accepted 22 August 2023

Keywords

Seismic design Fuzzy sets Fuzzification Fuzzy model Response spectrum

Abstract

The response spectra in the seismic design codes guide the seismic design force calculations that are crucial for structural safety and construction costs. In general, they are determined by crisp logic-based numerical classifications of seismic parameters, which primarily affect the shape and values of the spectrum. Crisp logic response spectra generation may have limitations in the accurate determination of relevant parameters. In this paper, a fuzzy inference system (FIS) rule-based model is proposed to address this issue. The proposed model uses spectral acceleration coefficients and shear wave velocity as inputs to generate the site coefficients of the response spectra according to the Türkiye Building Earthquake Code (TBEC 2018). The FIS model spectra generation is compared with the crisp logic model for thirtyfive examples, and the model performance is evaluated. The study demonstrates significant differences between the two models in terms of the response spectra' shape and acceleration spectrum intensity values, but the FIS model provides comparatively better accuracy in response spectra generation. The proposed model can be modified and applied to various parameters for generating response spectra in different seismic design codes with the exposition of fuzzy logic rules that show the concerned problem's internal working mechanism.

1. Introduction

Seismic design codes and provisions are utilized to withstand seismic loads during structural analysis [2-3]. Response spectra production for seismic design depends on several input parameters, including soil profiles, seismic zones, seismic coefficients, and site classes. These parameters significantly impact seismic design loads and play a crucial role in determining the appropriate structural system member type designs, dimensions, and materials. Accurate adaptation of parameters for response spectra generation is essential to minimize construction costs with structural safety insurance. Seismic design codes provide crisp logical parameter classifications, but the impact of fuzzification can be significant due to uncertainties in the design and computation stages. Fuzzification provides membership degrees (MDs) to account for uncertainties under the supervision of expert views for structural safety enhancement and construction cost optimization. Such an approach can alter the shape of the response spectrum and provide a plausible variation range in seismic load computations [4-6]. In practical earthquake engineering scenarios, the fuzzification of seismic coefficients has the potential to significantly alter the shape of the response spectrum and provide a range of

eISSN 2630-5763 © 2023 Authors. Publishing services by golden light publishing®.

^{*} Corresponding author (amangir@medipol.edu.tr)

plausible variations in final seismic load calculations. It is essential to compare different scenarios' results to include both crisp model values and fuzzy inference system (FIS) outputs. Thus, it is possible to assess the impact of fuzzification on the response spectrum shape and the corresponding seismic design loads. Such a comparison assists in determining the optimal method for better design performance improvement that helps to ensure seismic safety and cost-effectiveness in structural design. Since seismic forces consist of uncertainty types of vagueness, incompleteness, imprecision, bluntness and alike, fuzzy logic offers a more rational approach for predicting and minimizing the existing uncertainties in calculations. Hence, fuzzy logic can enhance the precision of seismic design and ensure adequate protection against seismic hazards.

Various studies have recently utilized fuzzy logic methods to integrate seismic effects by means of FIS modelling principles and how one can handle complexities, complications, uncertainties, and vagueness in lexical (verbal) statements [7-13]. Mellal [14] developed an approach for soil columns by merging fuzzy set theory and a nonlinear numerical model to obtain seismic response spectra. This FIS approach employed in the research enabled the quick determination of response spectra using fuzzy arithmetic on specific input parameters. Wadia-Fascetti and Güneş [15] incorporated statistical models to integrate fuzzy logic and quantify uncertainties in the structural response caused by ground motions. Ansari and Noorzad [16] suggested a fuzzy mathematics-based method to account for uncertainties in specific dynamic analysis parameters such as input excitation, stiffness, mass and damping in the response spectra of seismic activity in lowlands. Marano et al. [17] combined a probabilistic approach with fuzzy theory to define a ground motion model that generates a fuzzy classical stochastic response spectrum evaluation in linear systems.

Şen [18] proposed a rapid visual FIS computation model to categorize existing buildings for seismic hazard evaluation. Furthermore, Şen [19] presented another fuzzy classification method for identifying individual building hazard categories with different membership functions (MFs). On the other hand, Heidari and Khorasani [20] employed the Adaptive Neural Network Fuzzy Inference System (ANFIS) to produce synthetic earthquake accelerograms that comply with specific response spectra. The effectiveness of the proposed method is demonstrated through a set of illustrative recorded accelerograms. Ozkul et al. [21] presented a fuzzy degrading model that predicted the inelastic displacement ratios of reinforced concrete structures in dynamic analyses. This helps to specify the most suitable method for finding the degrading system displacement ratios. Bektaş and Kegyes-Brassai [22] proposed a rapid visual screening method with fuzzy logic for existing buildings in earthquake-prone zones based on 40 unreinforced masonry buildings data after the Albania Earthquake in 2019. Their fuzzy logic-based methods aim to identify building safety levels through computer algorithms such as artificial neural networks (ANNs), machine learning (ML), and fuzzy logic. Nahhas [23] and Mangir [24] developed different fuzzy models for seismic response spectra generation that complies with building codes. Besides these works, no open literature is currently available on acquiring seismic parameters for response spectra formation using fuzzy logic.

Various fuzzy logic-based methodologies are available for clustering multiple data, including hybrid fuzzy, adaptive neuro-fuzzy inference system (ANFIS), fuzzy cognitive mapping (FCM), and fuzzy decision tree (FDT), but their efficiency varies. Fuzzy cognitive maps (FCMs) and neuro-fuzzy inference systems (NFIS) are commonly utilized for clustering purposes [25]. FCMs also prove effective as decision-making tools in data management [26, 27]. In the context of three-dimensional coupled buildings under bi-directional seismic excitations, Al-Fahdawi and Barroso [28] introduced adaptive neuro-fuzzy and simple adaptive control methods. Ghani et al. [29] examined the earthquake-induced liquefaction behaviour of fine-grained soils using an artificial intelligence-based hybridized model that employs the adaptive neuro-fuzzy inference system. For predicting the seismic response of fibre-reinforced concrete columns, Mehrabi et al. [30] applied intelligent fuzzy-based hybrid metaheuristic techniques. Tombari and Stefanini [31] proposed a hybrid fuzzy-stochastic approach for one-dimensional site response analysis, incorporating probability models for seismic input and fuzzy intervals for soil uncertainties. Guo et al. [32] conducted an assessment of the seismic

vulnerability of reinforced concrete structures using global vulnerability curves and fuzzy theory. Fuzzy logic-based methods offer the advantage of capturing logical relationships between input and output variables, surpassing crisp logic methodologies. Moreover, these approaches help alleviate numerical and lexical uncertainties during the training and testing stages, resulting in more reliable verification and validation results. Nonetheless, one limitation of adaptive neuro-fuzzy inference systems pertains to their partially black-box behaviour concerning the internal generation mechanism of the system.

The main aim of this research is to develop a Fuzzy Inference System (FIS) model for certain input parameters to aid in the design of building-type structures in Türkiye according to the provisions of the current seismic design code (Türkiye Building Earthquake Code, TBEC 2018) [1]. Since TBEC 2018's rules are based on crisp logical deterministic principles, they lack uncertainties in the forms of imprecision and vagueness. The soil and seismic parameters of the response spectrum in TBEC 2018's standard regulation are fuzzified, and a FIS modelling approach is used to express the inherent uncertainties. Engineers and experts commonly rely on classical crisp classifications and mathematical equations as proposed in seismic design codes to adopt a response spectrum for seismic load computations in structural analysis and assessment procedures. The model proposed in this paper enhances to produce response spectra for various seismic codes leading to better accuracy and precision.

2. Türkiye Building Earthquake Code (2018) provisions

In most countries, multi-story building seismic design procedures depend on standard provisions included in the earthquake codes. Building inventory in Türkiye has a significant number of design and plan alternatives in the provisions of TBEC 2018 [1].

2.1. Earthquake ground motion levels

Four different earthquake ground motion levels are defined within the scope of TBEC 2018 [1] as DD-1, DD-2, DD-3 and DD-4. The DD-1 level earthquake is a seismic event that occurs very infrequently, with spectral magnitudes surpassed only once in the 50-year period corresponding to a 2% possibility of risk, resulting in a return period of 2475 years. This particular ground motion is also known as the maximum credible earthquake (MCE) that is taken into consideration. The DD-2 level earthquake represents an uncommon seismic event where spectral magnitudes surpass 50% within ten years, resulting in a recurrence interval of 475 years. This specific ground motion is recognized as the standard design earthquake. The DD-3 level earthquake is a common seismic event, with a 50% probability of spectral magnitude exceedance in 50 years, resulting in a return period of 72 years. Finally, the DD-4 level earthquake corresponds to the smallest ground motion, where spectral magnitudes are 68% likely to exceed 50 years (50% probability to exceed 30 years), and the corresponding return period is 43 years. After a DD-4 event, all buildings should continue their service without damage.

In general, in many design and assessment procedures, DD-2 level earthquake is considered for the calculation of the seismic load pattern on the buildings. Thus, the spectral values related to the DD-2 earthquake are used in this study.

2.2. Response spectra

The response spectra in TBEC 2018 [1] are provided with the methodology of horizontal elastic design spectral accelerations, S_{ae} (T) calculation, in gravitational acceleration (g) units, which are the ordinates of the horizontal elastic design acceleration spectrum for any earthquake ground motion level. These values are based on the natural vibration periods, T, in seconds (sec). The spectrum graph in Fig. 1 is obtained by the following set of equations. S_{DS} and S_{D1} indicate the design spectral acceleration coefficients at the short and 1.0 sec periods, respectively. T_A and T_B correspond to corner periods, and T_L is the transition of long-period.

$$S_{ae}(T) = \left(0.4 + 0.6 \frac{T}{T_A}\right) S_{DS} \qquad (0 \le T \le T_A)$$
 (1)

$$S_{ae}(T) = S_{DS} \qquad (T_A \le T \le T_B) \tag{2}$$

$$S_{ae}(T) = \frac{S_{D1}}{T} \qquad (T_B \le T \le T_L)$$
 (3)

$$S_{ae}(T) = \frac{S_{D1} T_L}{T^2} \qquad (T_L \le T)$$
 (4)

$$T_A = 0.2 \frac{S_{D1}}{S_{DS}}$$
 $T_B = \frac{S_{D1}}{S_{DS}}$ $T_L = 6 \text{ sec}$ (5)

2.2.1. Design spectral acceleration coefficients, S_{DS} and S_{D1}

Two design spectral acceleration coefficients, namely, S_{DS} and S_{D1} , are defined in the code for the generation of the response spectrum at the short and 1.0 sec periods, respectively. They are the products of the map spectral acceleration coefficients (S_S and S_1 ,) with site coefficients (F_S and F_1) as follows:

$$S_{DS} = S_S F_S \tag{6}$$

$$S_{D1} = S_1 F_1 \tag{7}$$

2.2.2. Map spectral acceleration coefficients, S_S and S_1

The map spectral acceleration coefficients, S_S and S_1 , corresponding to the geometric mean of earthquake effects in two perpendicular horizontal directions, are defined as dimensionless coefficients in the code at the short and 1.0 sec periods, respectively. They are found by dividing the map spectral accelerations by the gravitational acceleration for a 5% damping ratio based on the reference ground condition $[(V_S)_{30}=760 \text{ m/s}]$ for an earthquake ground motion level. $(V_S)_{30}$ is the average shear wave velocity of the soil beneath the foundation at the topmost 30 m layer. S_S and S_1 can be obtained from the earthquake hazard map of Türkiye. The related values are shown in Fig. 2 on this map for the DD-2 earthquake. This map is prepared by AFAD [33] based on the locations of the active fault lines, and colours on the map change according to the consideration of high-risk (purple) to low-risk (white) potential.

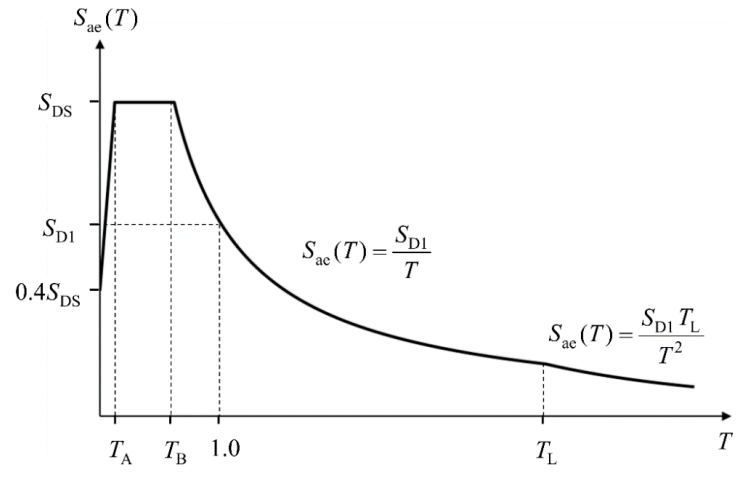


Fig. 1. The response spectrum, according to TBEC 2018 [1]

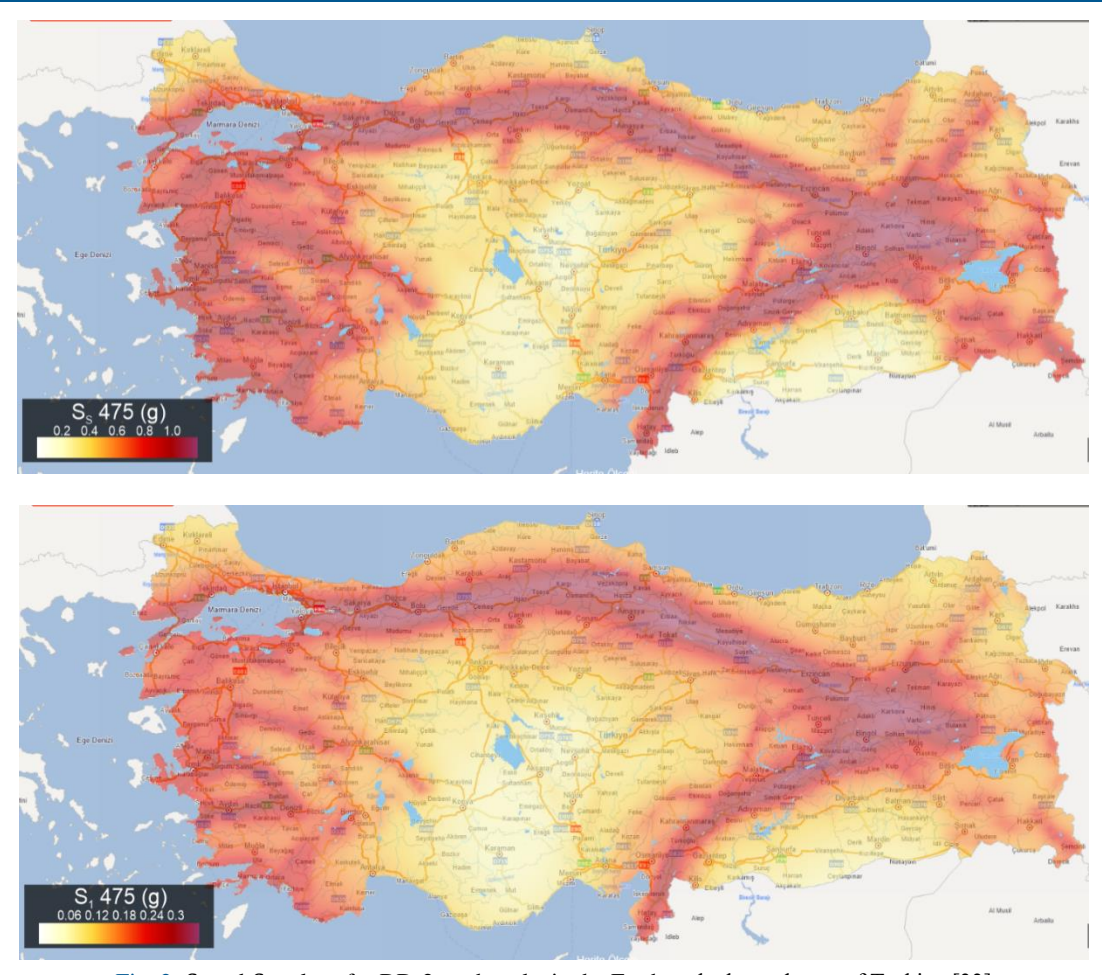


Fig. 2. S_S and S₁ values for DD-2 earthquake in the Earthquake hazard map of Türkiye [33]

2.2.3. Site coefficients, F_S and F_1

The site coefficients are F_5 and F_1 in TBEC 2018 [1] at the short and 1.0 sec periods, respectively. They are calculated using the values in Tables 1 and 2 by linear interpolation according to local soil classification and map spectral acceleration coefficients. Site-specific geotechnical investigations are necessary to specify the site coefficients of the "ZF" soil type.

2.3. Local soil classification

TBEC 2018 [1] provides a classification system for soil profiles based on the average shear wave velocity, $(V_S)_{30}$, of the soil profile beneath the foundation at the topmost 30 m layer. This classification system includes six local soil classes, namely, ZA, ZB, ZC, ZD, ZE, and ZF, that are characterized by generic linguistic descriptions in Table 3. It is important to note that the ZF soil type is susceptible to ground failure during earthquakes, and thus, site-specific geotechnical investigations are necessary to identify its seismic properties. Although the local soil classes are primarily associated with the average shear wave velocities, corresponding average standard penetration test (SPT) results, $(N_{60})_{30}$, and average undrained shear strength values, $(c_u)_{30}$, are also given in the same chart for soil class designation. Table 3 summarizes the local soil classes and their corresponding shear wave velocities, SPT test results, and undrained shear strength values in TBEC 2018 [1].

Table 1. Site coefficient at short period, Fs [1]

Level Coll Class	Site coefficient at the short period, F_S									
Local Soil Class	$S_{\rm S} \leq 0.25$	$S_S \leq 0.25$	$S_{\rm S} \leq 0.25$	$S_{\rm S} \leq 0.25$	$S_{\rm S} \leq 0.25$	$S_S \leq 0.25$				
ZA	0.8	0.8	0.8	0.8	0.8	0.8				
ZB	0.9	0.9 0.9		0.9	0.9	0.9				
ZC	1.3	1.3	1.3	1.3	1.3	1.3				
ZD	1.6	1.6	1.6	1.6	1.6	1.6				
ZE	2.4	2.4	2.4	2.4	2.4	2.4				
ZF		Site-specific	geotechnical inv	estigations shou	ıld be made.					

Table 2. Site coefficient at short period, F_S [1]

Land Call Class	Site coefficient at the 1.0 sec period, F_1									
Local Soil Class	S₁≤ 0.25	$S_1 \le 0.25$	$S_1 \le 0.25$	$S_1 \le 0.25$	$S_1 \le 0.25$	$S_1 \le 0.25$				
ZA	0.8	0.8	0.8	0.8	0.8	0.8				
ZB	0.8	0.8 0.8		0.8	0.8	0.8				
ZC	1.5	1.5	1.5	1.5	1.5	1.4				
ZD	2.4	2.2	2.0	1.9	1.8	1.7				
ZE	4.2	3.3	2.8	2.4	2.2	2.0				
ZF		Site-specific g	geotechnical inv	estigations show	ıld be made.					

Table 3. Local soil classes [1]

		Average value for the soil layer at the top 30 m								
Local Soil Class	Soil Type	$(V_S)_{30} (m/s)$	(N ₆₀) ₃₀ (blow/30 cm)	(c _u) ₃₀ (kPa)						
ZA	Solid, hard rocks.	> 1500	-	-						
ZB	Less weathered, moderately stiff rocks.	760 - 1500	-	-						
ZC	Very tight layers of sand, gravel and hard clay or weathered weak rocks with many cracks.	360 - 760	> 50	> 250						
ZD	Medium-firm layers of sand, gravel or very stiff clay layers.	180 - 360	15 - 50	70 - 250						
ZE	Profiles containing loose sand, gravel, or soft-solid clay layers or a total of more than 3 m thick, soft clay layer ($c_u < 25$ kPa) meeting PI >20 and w > 40% conditions.	< 180	< 15	< 70						
ZF	Soils that require site-specific investigation and evaluation:									
	1) Soils with the potential risk of failure and collapse under the influence of earthquakes (liquefiable soils, highly sensitive clays, collapsible weak cemented soils, etc.),									
	2) Clays with a total thickness of more than 3 m of peat and/or high organic content,									
	3) High plasticity clays (PI > 50) with a total thickness of more than 8 m,									
	4) Very thick (>35 m) soft or medium solid	l clays.								

3. Fuzzy inferencing (FIS) model

The Mamdani method [10-11] approach is used as the Fuzzy Inference System (FIS) that helps to determine site coefficients (F_S and F_1) of the response spectra as the model outputs. The model comprises two similar mechanisms: one for computing the short-period site coefficient, F_S , and the other for the site coefficient at 1.0 sec period, F_1 . Both mechanisms contain two input variables: the average shear wave velocity of the topmost 30 m soil layer (VS)30 and map spectral acceleration coefficients, S_S and S_1 , which differ depending on the short or 1.0 sec period values. SS is used as the second input for the estimation mechanism of FS, and S_1 is used for F_1 . The input and output variables are presented in fuzzy set forms, and a fuzzy logic rule base is established between the inputs and outputs for both mechanisms following the fuzzification of input variables. The output results are defuzzified to obtain crisp values for the site coefficients. The FIS model generates site coefficients by taking into account expert views concerning input variables' fuzzy sets to output fuzzy sets through a set of fuzzy rules. The fuzzy rule base establishes a connection between the fuzzy input sets and site coefficients for each rule considering the map spectral acceleration coefficient and soil class. These coefficients are then utilized to compute design spectral acceleration coefficients and generate fuzzy spectra.

The FIS model is implemented in MATLAB software [34] using the fuzzy logic controller tool to achieve high accuracy and practicality. The estimation mechanisms of the proposed FIS model for both site coefficients, F_S or F_1 , are illustrated in Fig. 3, which shows that some input and output MFs and rule bases are different for each site coefficient. Besides, the proposed FIS model is adaptable and can be used in other seismic design codes beyond TBEC 2018 [1]. This leads to more precise and accurate variables for seismic response spectrum estimation and generation.

3.1. Membership functions (MFs)

In the fuzzification procedures, trapezium and triangular MFs are considered for each input and output variable. As the common input variable for both FIS mechanisms, the soil classes are fuzzified based on the average shear wave velocity of the top 30 m soil layer $(V_S)_{30}$. Local soil classes and corresponding $(V_S)_{30}$ values in m/s units are described in detail under the local classification sub-section of Section 2. The fuzzy sets in the fuzzification of this input variable are like the MFs given by Nahhas [23]. The transition between peak shear wave velocity values is specified by triangular fuzzy sets. The shear wave velocity MFs connected to soil classes are shown in Fig. 4 as "ZE", "ZD", "ZC", "ZB", and "ZA". Since the "ZF" soil type requires a site-specific geotechnical survey, this soil type is not included within the scope of this study. The map spectral acceleration coefficients, S_S and S_1 , are fuzzified by considering the related table given in the code, as described in Section 2. Fig. 5 shows the MFs for S_S and S_1 input variables.

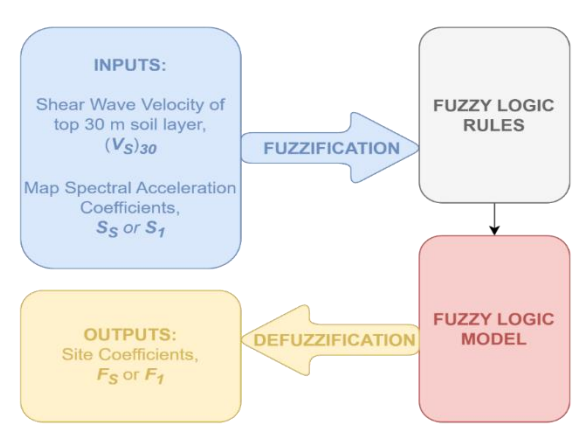


Fig. 3. The estimation mechanisms of the FIS model

In accordance with the code provisions in Section 2, the site coefficients, FS and F1, are classified into five inclusive fuzzy sets, namely, "Very Low", "Low", "Medium", "High", and "Very High". The MFs for these outputs are given in Fig. 6. The fuzzification process of input and output variables, shown in Fig. 4-6, involves trapezoidal MFs for the initial and final sets, along with various triangular MFs in between.

3.2. FIS and rule base

Expert opinions based on code provisions are helpful in generating a rule base establishment for a logical connection between input and output variables. The input variables have five to six MFs resulting in 30 combinations for the logical system of each MF in the fuzzy rule base (FRB), which are given in Fig. 4-5. Each rule in the FRB has a consistently consecutive standard structure as follows (see Tables 4 and 5 for more detail).

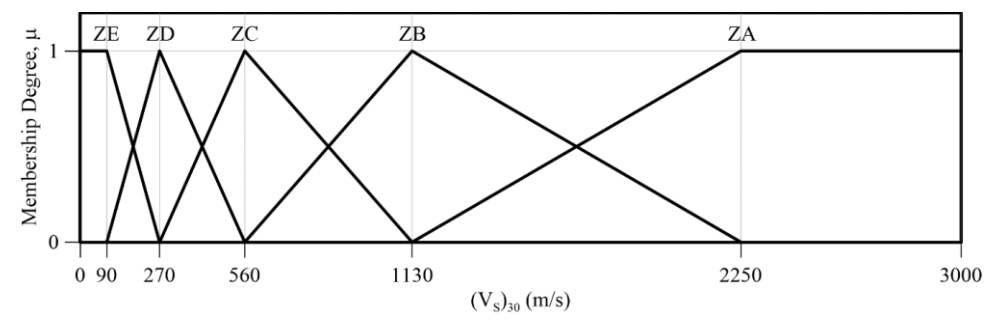


Fig. 4. Membership functions of average shear wave velocity at the topmost 30 m soil layer, $(V_S)_{30}$

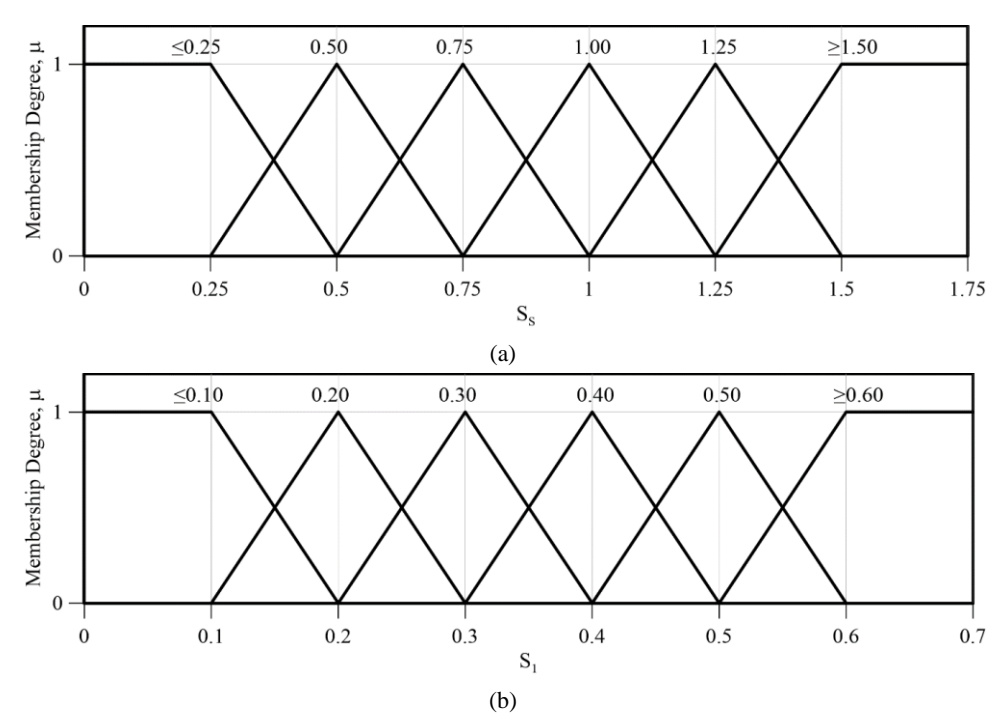


Fig. 5. Membership functions of the map spectral acceleration coefficients, (a) S_S and (b) S_1

289 Okumus and Mangir

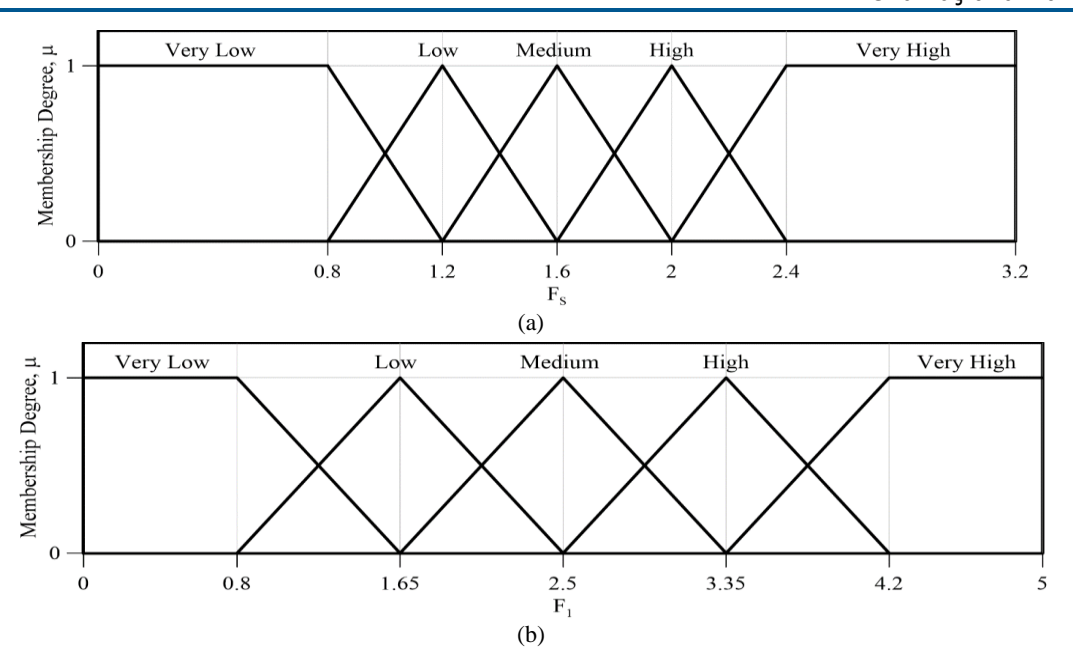


Fig. 5. Membership functions of the site coefficients, (a) F_S and (b) F_1

"IF soil class MF AND map spectral acceleration coefficient MF THEN site coefficient MF"

The rule base for the FIS model combines the input MFs using "AND"ing logical conjunction between the variables in each IF and THEN proposition. However, subsequent fuzzy rules are combined by "OR"ing logical conjunction. The FRBs for the proposed FIS model are shown in Tables 4 and 5. Each rule in the table represents a valid logical connection between input and output fuzzy MFs. In the proposed FIS model, the "MIN" inference corresponding to "AND"ing operator is used to combine input fuzzy sets and obtain the output result in each fuzzy rule.

On the other hand, the "MAX" operator corresponding "OR"ing fuzzy logical operation is used to aggregate the subsequent rules. Once the output is obtained in the form of a non-normal fuzzy set, a crisp value of the site coefficient is derived after the defuzzification of this fuzzy set for the design spectral acceleration coefficient calculation and the response spectrum generation. Defuzzification is achieved using the "Centroid" method [35]. The FIS rule base surface graphs in three dimensions for both site coefficients, F_S and F_1 , are shown in Fig. 7.

Table 4. Rule base of the site coefficient for the short period, F_S

```
IF "Soil Class" is "ZE" AND "SS" is "\( \leq 0.25\)" THEN "FS" is "Very High"
R1:
R2:
         IF "Soil Class" is "ZD" AND "SS" is "≤0.25" THEN "FS" is "Medium"
R3:
         IF "Soil Class" is "ZC" AND "SS" is "≤0.25" THEN "FS" is "Low"
R4:
         IF "Soil_Class" is "ZB" AND "SS" is "≤0.25" THEN "FS" is "Very Low"
R5
         IF "Soil Class" is "ZA" AND "SS" is "≤0.25" THEN "FS" is "Very Low"
         IF "Soil_Class" is "ZE" AND "SS" is "0.50" THEN "FS" is "High"
R6
R7
         IF "Soil_Class" is "ZD" AND "SS " is "0.50" THEN "FS" is "Medium"
         IF "Soil_Class" is "ZC" AND "SS" is "0.50" THEN "FS" is "Low"
R8:
         IF "Soil_Class" is "ZB" AND "SS" is "0.50" THEN "FS" is "Very Low"
R9:
R10:
         IF "Soil_Class" is "ZA" AND "SS" is "0.50" THEN "FS" is "Very Low"
```

Table 4. Continued

IF "Soil Class" is "ZE" AND "SS" is "0.75" THEN "FS" is "Low" R11: R12: IF "Soil Class" is "ZD" AND "SS" is "0.75" THEN "FS" is "Low" IF "Soil_Class" is "ZC" AND "SS" is "0.75" THEN "FS" is "Low" R13: R14: IF "Soil_Class" is "ZB" AND "SS" is "0.75" THEN "FS" is "Very Low" R15: IF "Soil_Class" is "ZA" AND "SS" is "0.75" THEN "FS" is "Very Low" R16: IF "Soil_Class" is "ZE" AND "SS" is "1.00" THEN "FS" is "Low" R17: IF "Soil_Class" is "ZD" AND "SS" is "1.00" THEN "FS" is "Low" R18: IF "Soil_Class" is "ZC" AND "SS" is "1.00" THEN "FS" is "Low" R19: IF "Soil_Class" is "ZB" AND "SS" is "1.00" THEN "FS" is "Very Low" R20: IF "Soil_Class" is "ZA" AND "SS" is "1.00" THEN "FS" is "Very Low" R21: IF "Soil_Class" is "ZE" AND "SS" is "1.25" THEN "FS" is "Very Low" R22: IF "Soil_Class" is "ZD" AND "SS" is "1.25" THEN "FS" is "Low" R23: IF "Soil_Class" is "ZC" AND "SS" is "1.25" THEN "FS" is "Low" R24: IF "Soil_Class" is "ZB" AND "SS" is "1.25" THEN "FS" is "Very Low" R25: IF "Soil_Class" is "ZA" AND "SS" is "1.25" THEN "FS" is "Very Low" R26: IF "Soil Class" is "ZE" AND "SS" is "≥1.50" THEN "FS" is "Very Low" R27: IF "Soil Class" is "ZD" AND "SS" is "≥1.50" THEN "FS" is "Low" IF "Soil Class" is "ZC" AND "SS" is "≥1.50" THEN "FS" is "Low" R28: R29: IF "Soil Class" is "ZB" AND "SS" is "≥1.50" THEN "FS" is "Very Low" R30: IF "Soil Class" is "ZA" AND "SS" is "≥1.50" THEN "FS" is "Very Low"

Table 5. Rule base of the site coefficient for the 1.0 sec period, F_1

R1:	IF "Soil_Class" is "ZE" AND "S1" is "≤0.10" THEN "F1" is "Very High"
R2:	IF "Soil_Class" is "ZD" AND "S1" is "≤0. 10" THEN "F1" is "Medium"
R3:	IF "Soil_Class" is "ZC" AND "S1" is "≤0. 10" THEN "F1" is "Low"
R4:	IF "Soil_Class" is "ZB" AND "S1" is "≤0. 10" THEN "F1" is "Very Low"
R5	IF "Soil_Class" is "ZA" AND "S1" is "≤0. 10" THEN "F1" is "Very Low"
R6	IF "Soil_Class" is "ZE" AND "S1" is "0.20" THEN "F1" is "High"
R7	IF "Soil_Class" is "ZD" AND "S1 " is "0.20" THEN "F1" is "Medium"
R8:	IF "Soil_Class" is "ZC" AND "S1" is "0.20" THEN "F1" is "Low"
R9:	IF "Soil_Class" is "ZB" AND "S1" is "0.20" THEN "F1" is "Very Low"
R10:	IF "Soil_Class" is "ZA" AND "S1" is "0.20" THEN "F1" is "Very Low"
R11:	IF "Soil_Class" is "ZE" AND "S1" is "0.30" THEN "F1" is "Medium"
R12	IF "Soil_Class" is "ZD" AND "S1" is "0.30" THEN "F1" is "Medium"
R13:	IF "Soil_Class" is "ZC" AND "S1" is "0.30" THEN "F1" is "Low"
R14:	IF "Soil_Class" is "ZB" AND "S1" is "0.30" THEN "F1" is "Very Low"
R15:	IF "Soil_Class" is "ZA" AND "S1" is "0.30" THEN "F1" is "Very Low"

Table 5. Continued

IF "Soil Class" is "ZE" AND "S1" is "0.40" THEN "F1" is "Medium" R16: R17: IF "Soil Class" is "ZD" AND "S1" is "0.40" THEN "F1" is "Low" R18: IF "Soil Class" is "ZC" AND "S1" is "0.40" THEN "F1" is "Low" R19: IF "Soil_Class" is "ZB" AND "S1" is "0.40" THEN "F1" is "Very Low" R20: IF "Soil_Class" is "ZA" AND "S1" is "0.40" THEN "F1" is "Very Low" R21: IF "Soil_Class" is "ZE" AND "S1" is "0.50" THEN "F1" is "Medium" R22: IF "Soil_Class" is "ZD" AND "S1" is "0.50" THEN "F1" is "Low" R23: IF "Soil_Class" is "ZC" AND "S1" is "0.50" THEN "F1" is "Low" R24: IF "Soil_Class" is "ZB" AND "S1" is "0.50" THEN "F1" is "Very Low" R25: IF "Soil_Class" is "ZA" AND "S1" is "0.50" THEN "F1" is "Very Low" R26: IF "Soil_Class" is "ZE" AND "S1" is "≥0.60" THEN "F1" is "Medium" R27: IF "Soil Class" is "ZD" AND "S1" is "≥0.60" THEN "F1" is "Low" R28: IF "Soil Class" is "ZC" AND "S1" is "≥0.60" THEN "F1" is "Low" R29: IF "Soil Class" is "ZB" AND "S1" is "≥0.60" THEN "F1" is "Very Low" R30: IF "Soil Class" is "ZA" AND "S1" is "≥0.60" THEN "F1" is "Very Low"

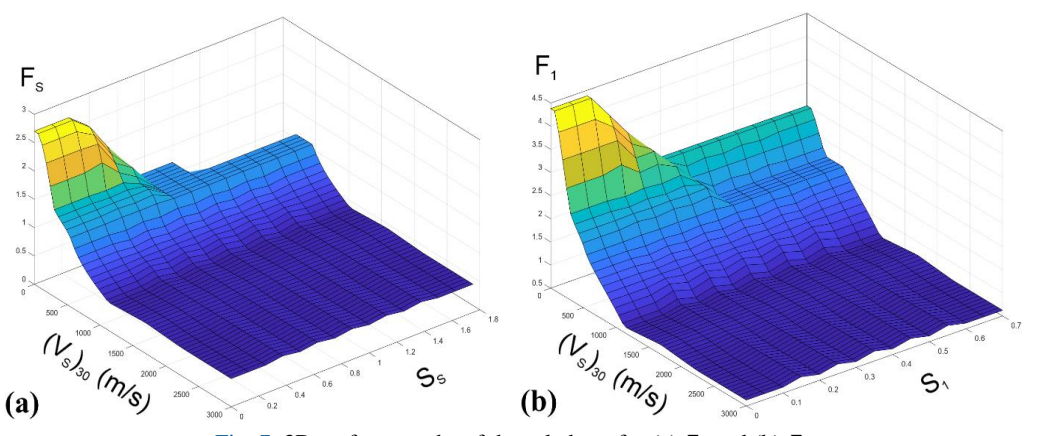


Fig. 7. 3D surface graphs of the rule base for (a) F_S and (b) F_1

4. Application

Thirty-five case scenarios are formed to evaluate the difference between response spectra generation by the crisp logic site coefficients in the code and the site coefficients obtained from the FIS model. The input data, including shear wave velocities $(V_S)_{30}$ and map spectral acceleration coefficients, S_S and S_1 , are determined for each case. Based on the TBEC 2018 [1] provisions in Section 2, the corresponding crisp site coefficients, F_S and F_1 , are calculated. Subsequently, according to the fuzzy model as described in Section 3, the fuzzy site coefficients, F_S' and F_1' , are also computed. After the crisp and fuzzy logic design spectral acceleration coefficients $(S_{SD}, S_{D1}, S_{SD}', S_{D1}')$ determination, the corresponding response spectra for each are generated by these values. In the calculations, various combinations are considered concerning soil profile types and map spectral acceleration values. The results are provided in Table 6, while Fig. 8~12 illustrate the results in graphical forms. Furthermore, the variation of peak ground acceleration (PGA) values of each case is compared and depicted in Fig. 13 with respect to shear wave velocities.

Гable 6.	Example of	case results									
Case	Soil	$*(V_S)_{30}$	Ss	S_1		TBEC-2018			Fuzzy Model		Difference (%)
No	Class	(m/s)	38	31	F_{S}	F_1	PGA (g)	F_{S}'	$F_1{}'$	PGA'(g)	PGA →PGA'
1	ZE	90	0.150	0.061	2.400	4.200	0.144	2.700	4.380	0.162	12.50%
2	ZE	105	0.400	0.141	1.980	3.831	0.317	2.350	3.850	0.376	18.61%
3	ZE	120	0.650	0.173	1.460	3.543	0.380	1.550	3.460	0.403	6.05%
4	ZE	135	0.850	0.218	1.220	3.210	0.415	1.200	3.100	0.408	-1.69%
5	ZE	150	1.100	0.291	1.020	2.845	0.449	0.804	2.610	0.354	-21.16%
6	ZE	165	1.350	0.318	0.860	2.728	0.464	0.697	2.290	0.376	-18.97%
7	ZE	180	1.600	0.461	0.800	2.278	0.512	0.743	2.080	0.476	-7.03%
8	ZD	180	0.150	0.061	1.600	2.400	0.096	2.290	3.460	0.137	42.71%
9	ZD	210	0.400	0.141	1.480	2.318	0.237	2.140	3.240	0.342	44.30%
10	ZD	240	0.650	0.173	1.280	2.254	0.333	1.460	2.950	0.380	14.11%
11	ZD	270	0.850	0.218	1.160	2.164	0.394	1.200	2.500	0.408	3.55%
12	ZD	300	1.100	0.291	1.060	2.018	0.466	1.200	2.380	0.528	13.30%
13	ZD	330	1.350	0.318	1.000	1.982	0.540	1.200	2.290	0.648	20.00%
14	ZD	360	1.600	0.461	1.000	1.839	0.640	1.200	1.650	0.768	20.00%
15	ZC	360	0.150	0.061	1.300	1.500	0.078	1.460	2.210	0.088	12.82%
16	ZC	427	0.400	0.141	1.300	1.500	0.208	1.390	2.050	0.222	6.73%
17	ZC	493	0.650	0.173	1.240	1.500	0.322	1.320	1.880	0.343	6.52%
18	ZC	560	0.850	0.218	1.200	1.500	0.408	1.200	1.650	0.408	0.00%
19	ZC	627	1.100	0.291	1.200	1.500	0.528	1.020	1.510	0.449	-14.96%
20	ZC	693	1.350	0.318	1.200	1.500	0.648	0.906	1.390	0.489	-24.54%
21	ZC	760	1.600	0.461	1.200	1.500	0.768	0.837	1.270	0.536	-30.21%
22	ZB	760	0.150	0.061	0.900	0.800	0.054	0.705	1.280	0.050	-7.41%

Continued	ļ									
ZB	883	0.400	0.141	0.900	0.800	0.144	0.629	1.070	0.113	-21.53%
ZB	1007	0.650	0.173	0.900	0.800	0.234	0.534	0.873	0.164	-29.91%
ZB	1130	0.850	0.218	0.900	0.800	0.306	0.534	0.653	0.182	-40.52%
ZB	1253	1.100	0.291	0.900	0.800	0.396	0.534	0.642	0.235	-40.66%
ZB	1377	1.350	0.318	0.900	0.800	0.486	0.528	0.660	0.288	-40.74%
ZB	1500	1.600	0.461	0.900	0.800	0.576	0.837	0.691	0.338	-41.32%
ZA	1500	0.150	0.061	0.800	0.800	0.048	0.528	0.680	0.032	-33.33%
ZA	1750	0.400	0.141	0.800	0.800	0.128	0.539	0.701	0.086	-32.81%
ZA	2000	0.650	0.173	0.800	0.800	0.208	0.534	0.669	0.139	-33.17%
ZA	2250	0.850	0.218	0.800	0.800	0.272	0.534	0.653	0.182	-33.09%
ZA	2500	1.100	0.291	0.800	0.800	0.352	0.534	0.638	0.235	-33.24%
ZA	2750	1.350	0.318	0.800	0.800	0.432	0.534	0.653	0.288	-33.33%
ZA	3000	1.600	0.461	0.800	0.800	0.512	0.499	0.691	0.319	-37.70%
	ZB ZB ZB ZB ZB ZA ZA ZA ZA ZA ZA	ZB 1007 ZB 1130 ZB 1253 ZB 1377 ZB 1500 ZA 1500 ZA 1750 ZA 2000 ZA 2250 ZA 2500 ZA 2750	ZB 883 0.400 ZB 1007 0.650 ZB 1130 0.850 ZB 1253 1.100 ZB 1377 1.350 ZB 1500 1.600 ZA 1500 0.150 ZA 1750 0.400 ZA 2000 0.650 ZA 2250 0.850 ZA 2500 1.100 ZA 2750 1.350	ZB 883 0.400 0.141 ZB 1007 0.650 0.173 ZB 1130 0.850 0.218 ZB 1253 1.100 0.291 ZB 1377 1.350 0.318 ZB 1500 1.600 0.461 ZA 1500 0.150 0.061 ZA 1750 0.400 0.141 ZA 2000 0.650 0.173 ZA 2250 0.850 0.218 ZA 2500 1.100 0.291 ZA 2750 1.350 0.318	ZB 883 0.400 0.141 0.900 ZB 1007 0.650 0.173 0.900 ZB 1130 0.850 0.218 0.900 ZB 1253 1.100 0.291 0.900 ZB 1377 1.350 0.318 0.900 ZB 1500 1.600 0.461 0.900 ZA 1500 0.150 0.061 0.800 ZA 1750 0.400 0.141 0.800 ZA 2000 0.650 0.173 0.800 ZA 2250 0.850 0.218 0.800 ZA 2500 1.100 0.291 0.800 ZA 2750 1.350 0.318 0.800	ZB 883 0.400 0.141 0.900 0.800 ZB 1007 0.650 0.173 0.900 0.800 ZB 1130 0.850 0.218 0.900 0.800 ZB 1253 1.100 0.291 0.900 0.800 ZB 1377 1.350 0.318 0.900 0.800 ZB 1500 1.600 0.461 0.900 0.800 ZA 1500 0.150 0.061 0.800 0.800 ZA 1750 0.400 0.141 0.800 0.800 ZA 2000 0.650 0.173 0.800 0.800 ZA 2250 0.850 0.218 0.800 0.800 ZA 2500 1.100 0.291 0.800 0.800 ZA 2750 1.350 0.318 0.800 0.800	ZB 883 0.400 0.141 0.900 0.800 0.144 ZB 1007 0.650 0.173 0.900 0.800 0.234 ZB 1130 0.850 0.218 0.900 0.800 0.306 ZB 1253 1.100 0.291 0.900 0.800 0.396 ZB 1377 1.350 0.318 0.900 0.800 0.486 ZB 1500 1.600 0.461 0.900 0.800 0.576 ZA 1500 0.150 0.061 0.800 0.800 0.048 ZA 1750 0.400 0.141 0.800 0.800 0.128 ZA 2000 0.650 0.173 0.800 0.800 0.208 ZA 2250 0.850 0.218 0.800 0.800 0.352 ZA 2500 1.100 0.291 0.800 0.800 0.432	ZB 883 0.400 0.141 0.900 0.800 0.144 0.629 ZB 1007 0.650 0.173 0.900 0.800 0.234 0.534 ZB 1130 0.850 0.218 0.900 0.800 0.306 0.534 ZB 1253 1.100 0.291 0.900 0.800 0.396 0.534 ZB 1377 1.350 0.318 0.900 0.800 0.486 0.528 ZB 1500 1.600 0.461 0.900 0.800 0.576 0.837 ZA 1500 0.150 0.061 0.800 0.800 0.048 0.528 ZA 1750 0.400 0.141 0.800 0.800 0.128 0.539 ZA 2000 0.650 0.173 0.800 0.800 0.208 0.534 ZA 2250 0.850 0.218 0.800 0.800 0.352 0.534 ZA 2500 1.100 0.291 0.800 0.800 0.432 0.534 ZA<	ZB 883 0.400 0.141 0.900 0.800 0.144 0.629 1.070 ZB 1007 0.650 0.173 0.900 0.800 0.234 0.534 0.873 ZB 1130 0.850 0.218 0.900 0.800 0.306 0.534 0.653 ZB 1253 1.100 0.291 0.900 0.800 0.396 0.534 0.642 ZB 1377 1.350 0.318 0.900 0.800 0.486 0.528 0.660 ZB 1500 1.600 0.461 0.900 0.800 0.576 0.837 0.691 ZA 1500 0.150 0.061 0.800 0.800 0.048 0.528 0.680 ZA 1750 0.400 0.141 0.800 0.800 0.128 0.539 0.701 ZA 2000 0.650 0.173 0.800 0.800 0.208 0.534 0.669 ZA 2250 0.850 0.218 0.800 0.800 0.352 0.534 0.653 <	ZB 883 0.400 0.141 0.900 0.800 0.144 0.629 1.070 0.113 ZB 1007 0.650 0.173 0.900 0.800 0.234 0.534 0.873 0.164 ZB 1130 0.850 0.218 0.900 0.800 0.306 0.534 0.653 0.182 ZB 1253 1.100 0.291 0.900 0.800 0.396 0.534 0.642 0.235 ZB 1377 1.350 0.318 0.900 0.800 0.486 0.528 0.660 0.288 ZB 1500 1.600 0.461 0.900 0.800 0.576 0.837 0.691 0.338 ZA 1500 0.150 0.061 0.800 0.800 0.048 0.528 0.680 0.032 ZA 1750 0.400 0.141 0.800 0.800 0.128 0.539 0.701 0.086 ZA 2250 0.850 0.218 0.800 0.800 0.272 0.534 0.653 0.182

^{*} Input values used in the FIS model

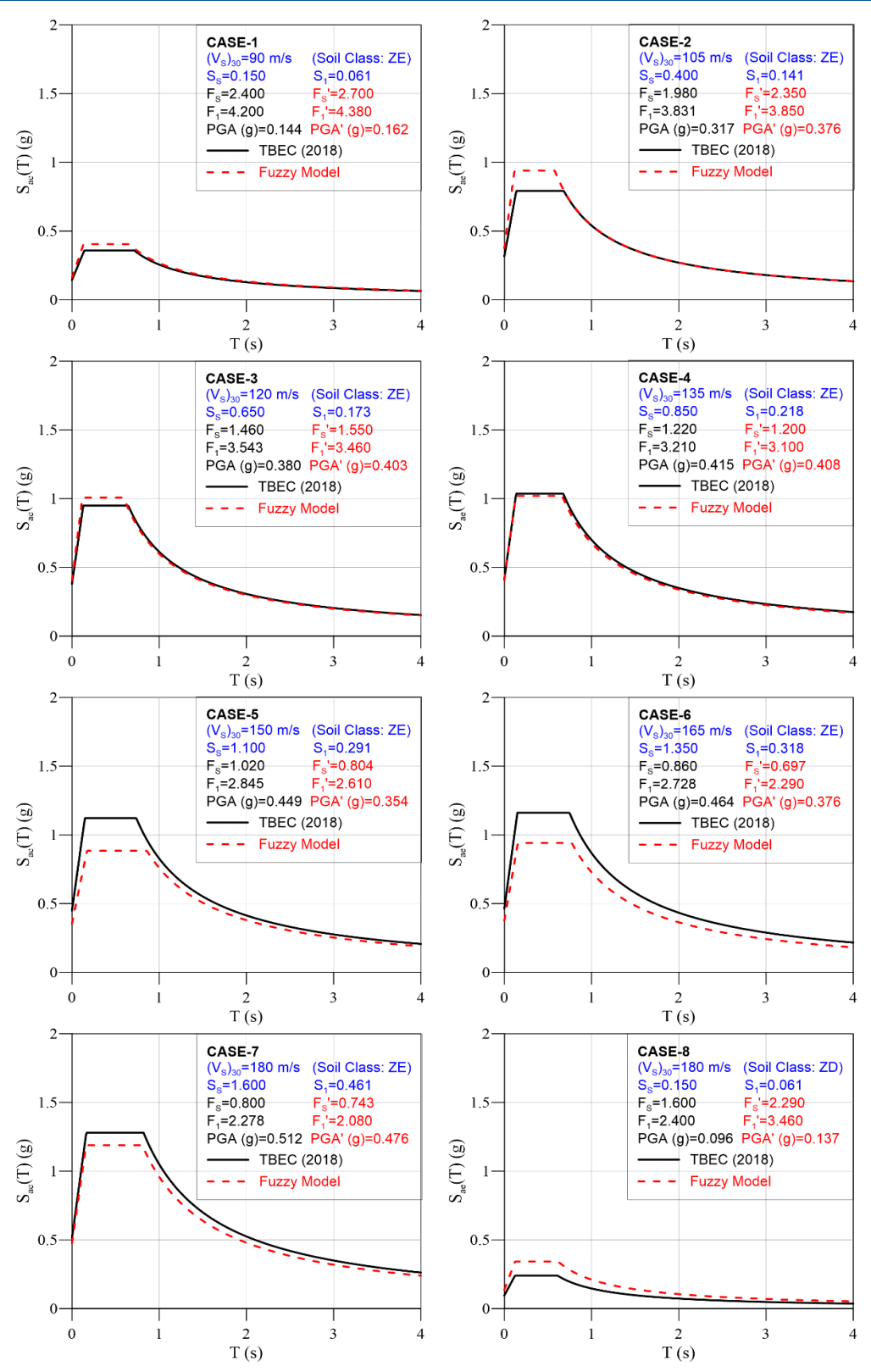


Fig. 8. TBEC 2018 [1] vs fuzzy response spectra; case 1~8

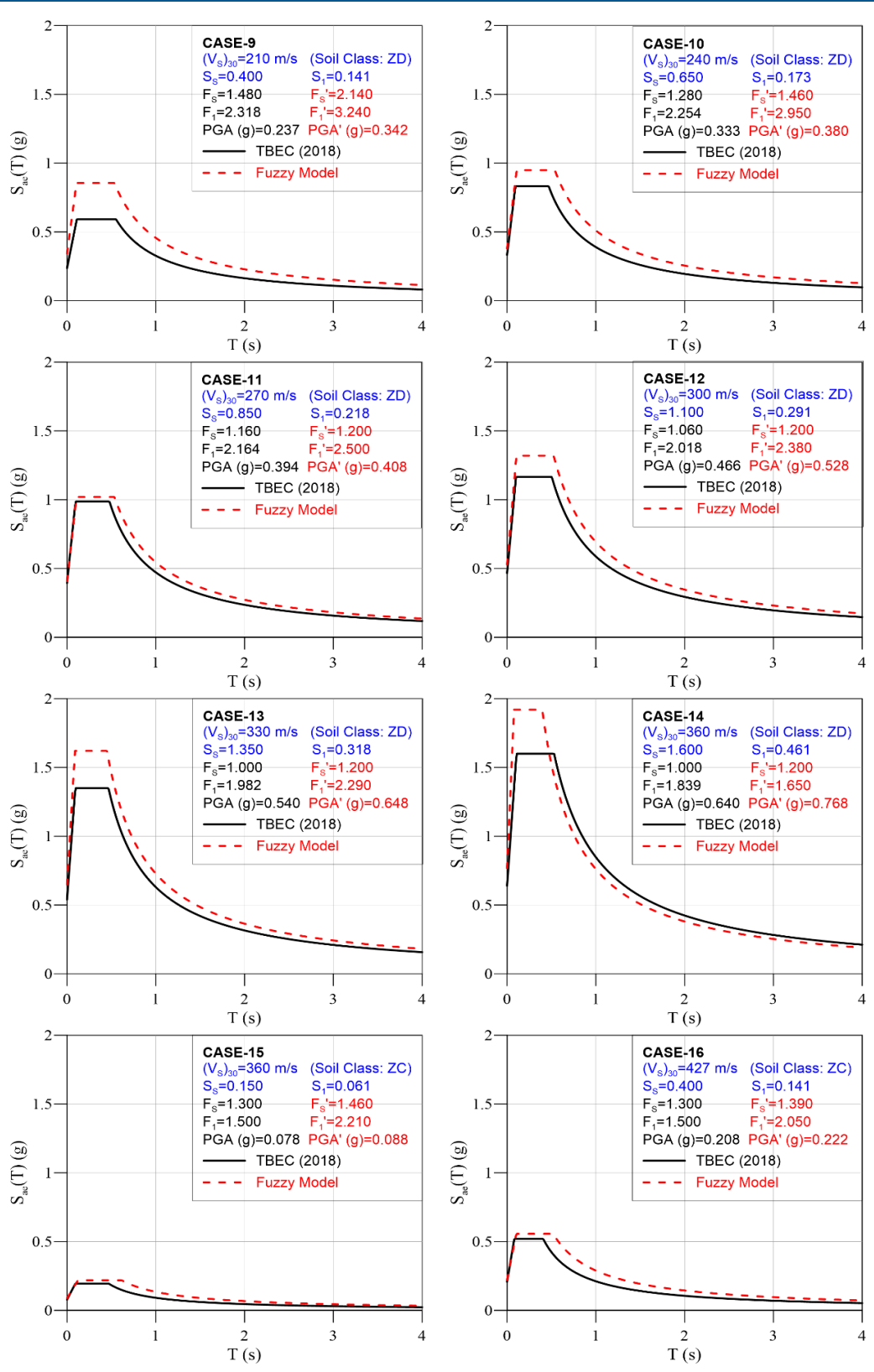


Fig. 9. TBEC 2018 [1] vs fuzzy response spectra; case 9~16

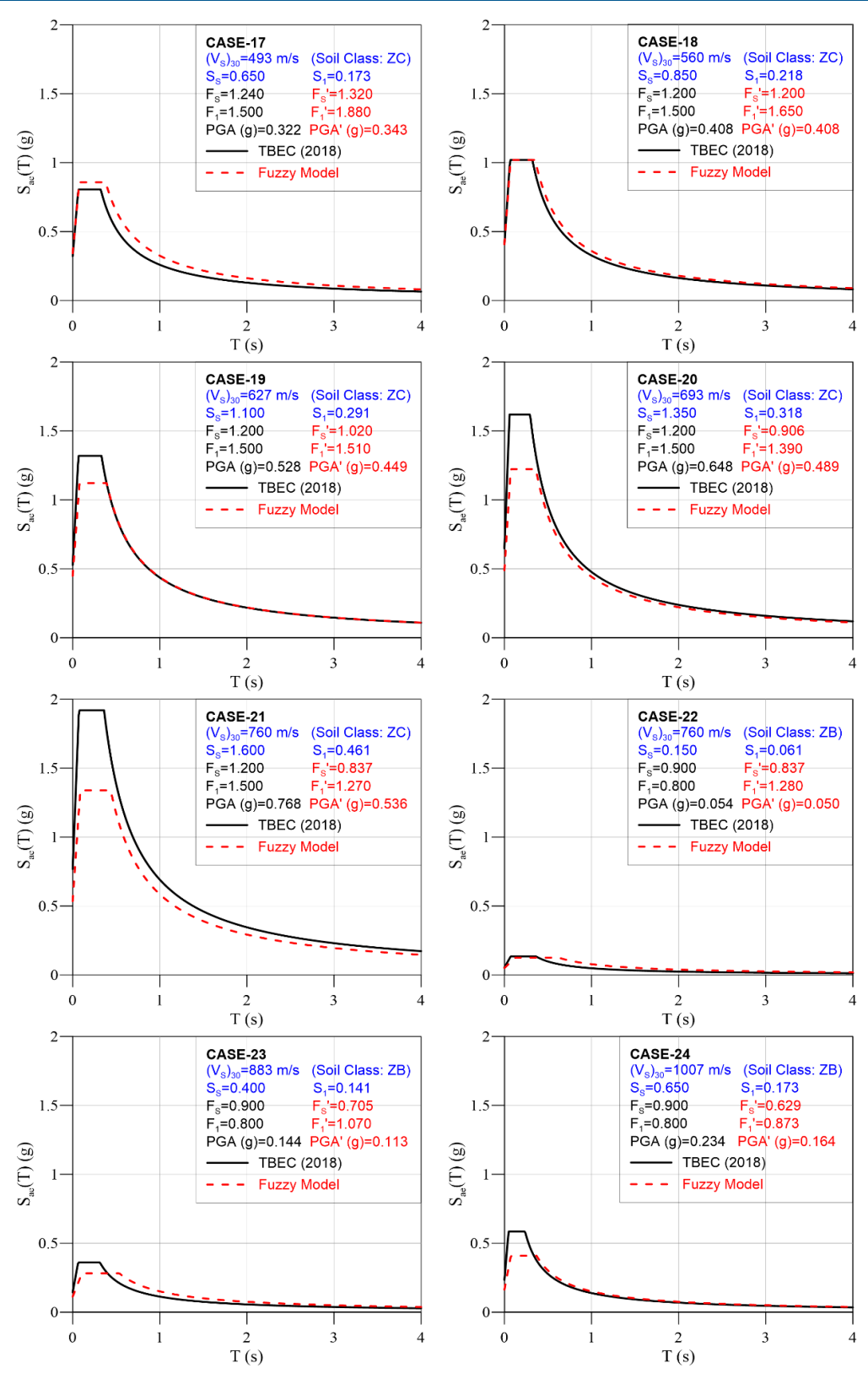


Fig. 10. TBEC 2018 [1] vs fuzzy response spectra; case 17~24

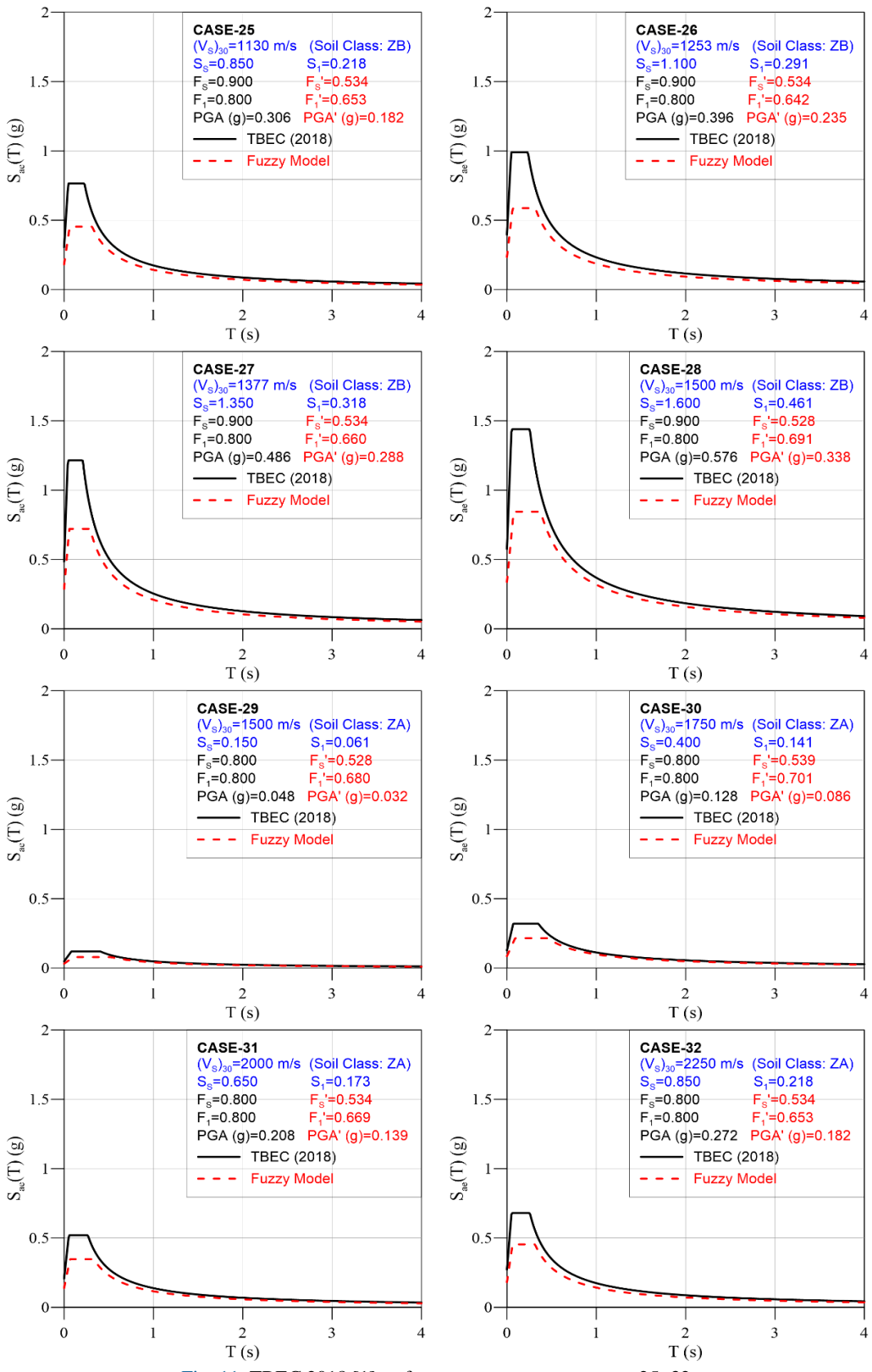


Fig. 11. TBEC 2018 [1] vs fuzzy response spectra; case 25~32

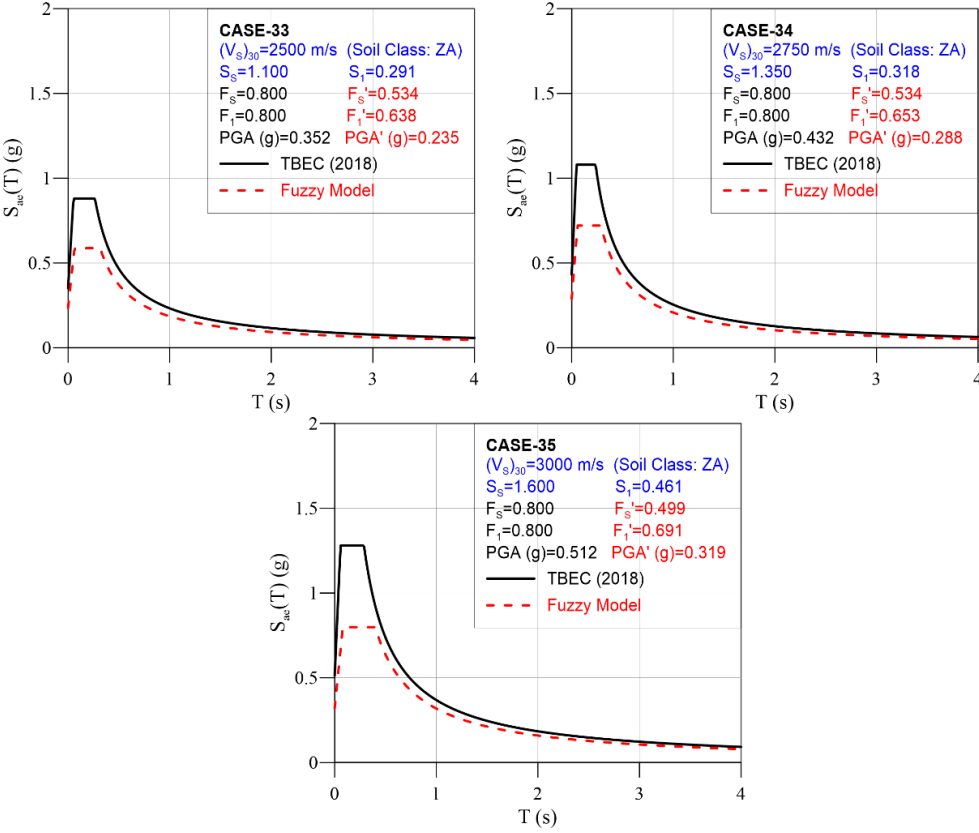


Fig. 12. TBEC 2018 [1] vs fuzzy response spectra; case 33~35

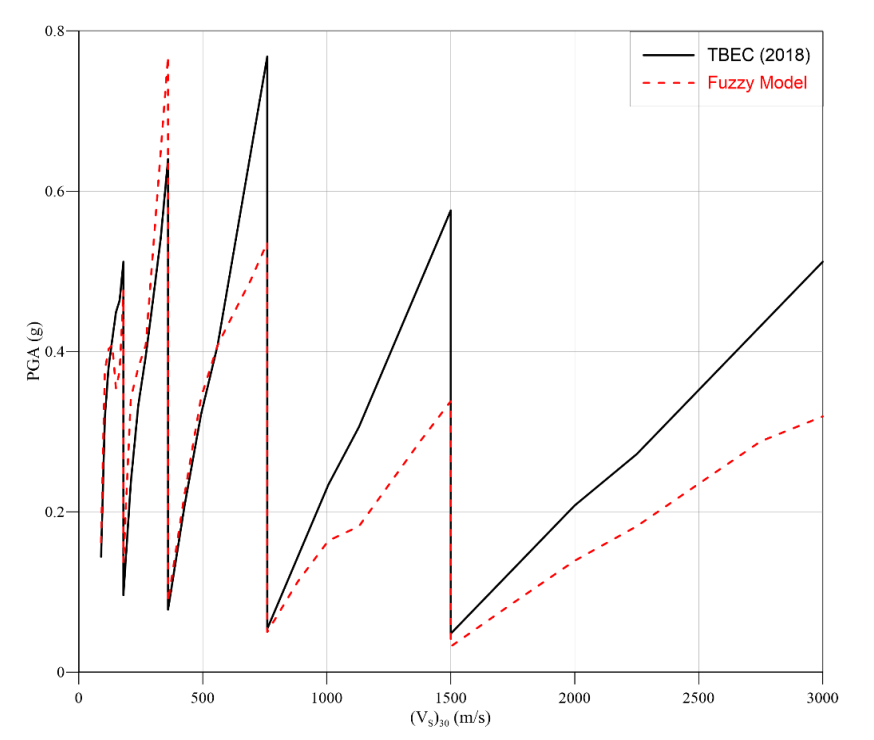


Fig. 13. The variation of peak ground acceleration values with respect to $(V_S)_{30}$

According to Oğuz [36], the acceleration spectrum intensity provides an indication of the potential damage caused by strong ground motions. The extent of damage in a specific region is represented by the area under the response spectrum within a given period range. Travasarou et al. [37] established a strong relationship between the displacement demand from an earthquake and the acceleration spectrum intensities. In order to compare the damage potential, these intensities are calculated for all example cases, and the results are given in Table 7. Fig. 14 displays the areas (spectrum intensities) under various regions on an example acceleration spectrum graph. The peak ground acceleration (PGA) represents the first acceleration value at the 0 sec period. A_T denotes the total area of the spectrum, known as the acceleration spectrum intensity. A_1 , A_2 , and A_3 represent the areas of the increasing acceleration, constant acceleration, and constant velocity regions, respectively.

5. Discussion

Response spectrum generation by the FIS model reveals that spectra intensity and shape can be affected according to the basic information availability. There are differences between the code response spectrum and the FIS response spectrum. The maximum acceleration value of the spectrum that shows the spectral acceleration value at the constant acceleration region of the spectrum, namely the peak spectral acceleration (PSA), equals S_{DS} and is directly proportional to the peak ground acceleration (PGA), corresponding to 0.4 S_{DS} . Therefore, comparisons related to PGA values are also valid for the PSA values. PGA values are used in comparisons.

The FIS-based spectrum for the ZE soil class tends to provide lower spectral acceleration values with increasing map spectral acceleration coefficients (Fig. 8, from Case 1 to Case 7). For Case 5, PGA is decreased by 21% in the FIS-based spectrum. Also, A1 and A2 regions tend to become narrower, giving a much lower spectral intensity, especially for the medium map spectral acceleration coefficients as in Fig. 8 for Cases 5 and 6. The maximum difference between the total spectrum intensity is 7% for the lower map spectral acceleration coefficients, providing higher intensity values for the FIS-based spectra. However, the maximum difference is -17% for the higher map spectral acceleration coefficients, meaning that the FIS-based spectra result in lower spectral acceleration values.

In the cases of the ZD soil class, the FIS-based spectra provided higher spectral accelerations in almost all cases for the whole period range except Case 14. The highest difference in PGA is obtained in Case 9 with a 44% value. Including Case 14, all ZD cases provided higher spectral accelerations for the A1 and A2 regions. The difference between the crisp and FIS-based spectrum intensities appears to be up to 44%. The total spectrum intensity difference is much higher in the lower map spectral acceleration coefficient cases and eventually drops around zero at the highest map spectral acceleration coefficient case.

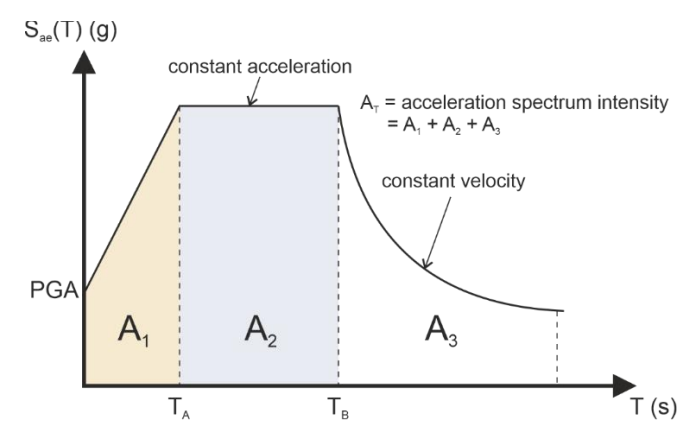


Fig. 14. Calculation procedures of the acceleration spectrum intensity

Table 7. Comparisons for the acceleration spectrum intensities

Case No			Accele	eration Spe		D:66	(0/)							
		TBEC-2	2018 [1]			Fuzzy Model				Differences (%)				
	A ₁	A ₂	A ₃	AT	A ₁ '	A ₂ '	A ₃ '	A _T '	$A_1 \rightarrow A_1'$	$A_2 \rightarrow A_2'$	A ₃ →A ₃ '	$A_T \rightarrow A_T'$		
1	0.0350	0.2052	0.4429	0.6831	0.0366	0.2146	0.4814	0.7327	5%	5%	9%	7%		
2	0.0784	0.4277	0.9572	1.4633	0.0802	0.4324	1.0483	1.5608	2%	1%	10%	7%		
3	0.0866	0.4934	1.1138	1.6938	0.0950	0.4635	1.1456	1.7041	10%	-6%	3%	1%		
4	0.0929	0.5599	1.2503	1.9031	0.0921	0.5405	1.2177	1.8503	-1%	-3%	-3%	-3%		
5	0.1186	0.6620	1.3970	2.1776	0.1048	0.6102	1.1675	1.8824	-12%	-8%	-16%	-14%		
6	0.1221	0.6966	1.4522	2.2709	0.0975	0.5833	1.1998	1.8806	-20%	-16%	-17%	-17%		
7	0.1418	0.8447	1.6642	2.6508	0.1327	0.7727	1.5314	2.4367	-6%	-9%	-8%	-8%		
8	0.0200	0.1176	0.2753	0.4129	0.0286	0.1683	0.3969	0.5938	43%	43%	44%	44%		
9	0.0455	0.2605	0.6485	0.9545	0.0667	0.3595	0.9233	1.3496	47%	38%	42%	41%		
10	0.0515	0.3160	0.8350	1.2026	0.0737	0.4081	1.0220	1.5038	43%	29%	22%	25%		
11	0.0702	0.3747	1.0003	1.4451	0.0794	0.4284	1.1015	1.6094	13%	14%	10%	11%		
12	0.0814	0.4664	1.2211	1.7688	0.0905	0.5542	1.4130	2.0577	11%	19%	16%	16%		
13	0.0837	0.5128	1.3496	1.9462	0.1021	0.5832	1.5910	2.2763	22%	14%	18%	17%		
14	0.1250	0.6720	1.7135	2.5106	0.1079	0.6143	1.7515	2.4737	-14%	-9%	2%	-1%		
15	0.0121	0.0741	0.1959	0.2821	0.0182	0.1095	0.2513	0.3790	51%	48%	28%	34%		
16	0.0289	0.1716	0.4818	0.6823	0.0383	0.2335	0.5897	0.8615	32%	36%	22%	26%		
17	0.0329	0.2094	0.6554	0.8977	0.0490	0.2574	0.7656	1.0720	49%	23%	17%	19%		
18	0.0417	0.2650	0.8259	1.1326	0.0498	0.2856	0.8763	1.2117	20%	8%	6%	7%		
19	0.0661	0.3432	1.0891	1.4983	0.0633	0.3478	1.0229	1.4341	-4%	1%	-6%	-4%		
20	0.0685	0.3726	1.2517	1.6927	0.0591	0.3546	1.0644	1.4781	-14%	-5%	-15%	-13%		
21	0.0929	0.5566	1.6651	2.3147	0.0853	0.4687	1.2923	1.8463	-8%	-16%	-22%	-20%		

Table 7. C	Continued											
22	0.0065	0.0391	0.1175	0.1632	0.0104	0.0628	0.1456	0.2187	59%	60%	24%	34%
23	0.0148	0.0900	0.2885	0.3933	0.0220	0.1212	0.3021	0.4453	48%	35%	5%	13%
24	0.0209	0.1111	0.3894	0.5214	0.0196	0.1226	0.3595	0.5017	-6%	10%	-8%	-4%
25	0.0277	0.1377	0.4981	0.6634	0.0187	0.1134	0.3641	0.4962	-32%	-18%	-27%	-25%
26	0.0354	0.1880	0.6550	0.8784	0.0241	0.1526	0.4719	0.6486	-32%	-19%	-28%	-26%
27	0.0334	0.2064	0.7498	0.9895	0.0306	0.1658	0.5508	0.7472	-8%	-20%	-27%	-24%
28	0.0930	0.2591	1.0081	1.3602	0.0484	0.2534	0.7498	1.0516	-48%	-2%	-26%	-23%
29	0.0067	0.0396	0.1112	0.1574	0.0054	0.0333	0.0846	0.1233	-19%	-16%	-24%	-22%
30	0.0156	0.0896	0.2748	0.3800	0.0135	0.0798	0.2138	0.3070	-14%	-11%	-22%	-19%
31	0.0177	0.1143	0.3731	0.5051	0.0173	0.0902	0.2887	0.3963	-2%	-21%	-23%	-22%
32	0.0235	0.1427	0.4767	0.6430	0.0187	0.1134	0.3641	0.4962	-21%	-21%	-24%	-23%
33	0.0301	0.1847	0.6363	0.8510	0.0241	0.1526	0.4689	0.6457	-20%	-17%	-26%	-24%
34	0.0386	0.2051	0.7158	0.9595	0.0307	0.1658	0.5449	0.7414	-20%	-19%	-24%	-23%
35	0.0546	0.2944	0.9678	1.3167	0.0448	0.2555	0.7335	1.0337	-18%	-13%	-24%	-21%

In the cases of ZC soil class, a strong correlation exists between the code and FIS-based spectra for the lower map spectral acceleration coefficients. As the map spectral acceleration coefficients increase, code-based spectra result in significantly higher values for the constant acceleration region. In Case 21, the FIS-based spectrum provided a 30% lower PGA. A decrease in total spectrum intensities with the increase in the map spectral acceleration coefficients is evident for ZC soil class. The variation in the total spectrum intensity is 34% for lower map spectral acceleration coefficient cases, but this difference drops down to -20% for the higher map spectral acceleration coefficient cases. It is important to note that the FIS-based spectra provide up to 51% higher spectrum intensity values in the A₁ and A₂ regions.

In stiffer soils, although spectral acceleration results are quite compatible at the long period range of the spectra, the code-based spectra result in higher spectral accelerations than the FIS-based ones in the A_1 and A_2 regions. This outcome can be seen for the ZB class in Fig. 10 (from Case 22 to Case 24) and 11 (from Case 25 to Case 28), which is clearly visible in the higher map spectral acceleration coefficient cases. In Case 28, the PGA of FIS-based spectra is 41% lower than the crisp one. The FIS-based spectra provide higher spectrum intensity values in A_1 (59%) and A_2 regions (60%). However, the FIS-based spectra result in lower intensity values with increasing map spectral acceleration coefficients. When the total spectrum intensity values are compared, the FIS-based spectra provide lower values of up to 26%.

Higher spectral accelerations are also apparent for stiff soils in the ZA soil class cases. The code-based spectra provide higher spectral accelerations in all ZA cases, especially for the A_1 and A_2 regions. In Case 35, the FIS-based spectrum provided a 37% lower PGA than the crisp one. In line with this outcome, spectrum intensities are also found to be lower for the FIS-based spectra in all spectrum regions. The FIS-based spectra result in up to 24% lower total spectrum intensity values than the code-based ones.

6. Conclusion

The fuzzy logic inference system (FIS) model is a valuable tool for addressing linguistic uncertainties by utilizing fuzzy sets. It has been widely applied in various fields to handle uncertainties such as imprecision, vagueness, and incompleteness in data. In contrast to the deterministic classification of seismic codes, the proposed FIS model for response spectra methodology considers the imperfections associated with soil class selection and the map spectral acceleration values. In this paper, the site coefficients from the current seismic design code of Türkiye [1] provisions are employed for thirty-five different example cases with varying soil classes, shear wave velocities, and map spectral acceleration values. A comparison between the fuzzy and crisp logic output seismic parameters revealed significant differences in the response spectra' shape and the acceleration spectrum intensity values.

In some cases with various soil classes, the response spectra by the FIS model tend to result in higher spectral acceleration values than traditional response spectra. The implication of this observation is that the design acceleration values specified by the code may not provide enough structural safety, taking into account the uncertainties present at those locations. Conversely, in some other cases, the FIS model response spectra yield comparable or lower values than the traditional ones, suggesting that the traditional response spectra might lead to higher design requirements for structures complying with the building code. As a result, incorporating the fuzzy version of the response spectrum has the potential to provide a design solution that could be safer or more cost-effective in different scenarios, considering the uncertain nature of the soil profile and vagueness of the map spectral accelerations and site coefficients.

The differences between the total spectrum intensities were found to vary from 1% up to 44%, and the differences between the PGA values were found to be 0%~44% in various cases. A regular change pattern is hard to conduct based on the differences in PGA and spectrum intensity values. However, code-based spectra strongly tend to provide higher PGA values and intensities with increasing soil stiffness. The FIS-based spectra provided significant differences in soft soils, especially for short periods. Fuzzy-based spectra

yielded higher map spectral acceleration values from 0.15 to 0.65 range in S_s and from 0.06 to 0.17 range in S_1 for the ZE soil class. Similarly, the fuzzy-based spectra provided higher values in almost all map spectral accelerations for the ZD soil class. Therefore, when there is a suspicion of soft soil presence or uncertain seismic parameters, using the fuzzy-based spectrum might be an alternative for comparing with the code-based spectrum to provide more structural safety. Although the highest differences are obtained from short and medium-period regions, it is possible to say that the long-period spectral accelerations are also affected strongly in some cases. Thus, the FIS model could be an alternative tool to produce a fuzzy spectrum to check the design approach of code-based spectrum considering the uncertainties in the soil profile, structural safety, and cost-effectiveness.

The utilization of a FIS model aids in the generation of response spectra that better capture the inherent uncertainties in the problem, resulting in designs that are more resilient and dependable. Moreover, this approach can also be applied to investigate the seismic parameters of alternative design codes. However, further extensive research is required to gain a complete understanding of the potential and constraints associated with the FIS model.

Conflict of interests

The author(s) declared no potential conflicts of interest with respect to the research, authorship, and/or publication of this article.

Funding

This research received no external funding.

Data availability statement

No new data were created or analyzed in this study.

References

- [1] TBEC (2018) Türkiye Building Earthquake Code. Disaster and Emergency Management Presidency, Ministry of Interior. Ankara, Türkiye.
- [2] Mohraz B, Sadek F (2001) Earthquake Ground Motion and Response Spectra. In: Naeim F (ed) The Seismic Design Handbook. Springer Boston MA, Inc., pp. 47-124.
- [3] Trifunac MD (2012) Earthquake response spectra for performance-based design-A critical review. Soil Dynamics & Earthquake Engineering 37:73-83.
- [4] Goulet CA, Haselton CB, Mitrani-Reiser J, Beck JL, Deierlein GG, Porter KA, Stewart JP (2007) Evaluation of the seismic performance of a code-conforming reinforced-concrete frame building from seismic hazard to collapse safety and economic losses. Earthquake Engineering & Structural Dynamics 36(13):1973-1997.
- [5] Mitropoulou CC, Lagaros ND, Papadrakakis M (2011) Life-cycle cost assessment of optimally designed reinforced concrete buildings under seismic actions. Reliability Engineering & System Safety 96(10):1311-1331.
- [6] Ramirez CM, Liel AB, Mitrani-Reiser J, Haselton CB, Spear AD, Steiner J, Deierlein GG, Miranda E (2012) Expected earthquake damage and repair costs in reinforced concrete frame buildings. Earthquake Engineering & Structural Dynamics 41(11):1455-1475.
- [7] Zadeh LA (1965) Fuzzy sets. Information and Control 8(3):338–353.
- [8] Zadeh LA (1973) Outline of a new approach to the analysis of complex systems and decision processes. IEEE Transactions on Systems Man and Cybernetics 3:28–44.
- [9] Zadeh LA (1975) The concept of a linguistic variable and its application to approximate reasoning, Parts I, II, III. Information Science 8(4):199–249,301–357,43–80.
- [10] Mamdani EH (1974) Application of fuzzy algorithms for simple dynamic plant. In: Proceedings of the IEEE 121:1585–1588.

- [11] Mamdani EH, Assilian S (1975) An experiment in linguistic synthesis with a fuzzy logic controller. International Journal of Man-Machine Studies 7(1):1–13.
- [12] Sugeno M (1985) Industrial Applications of Fuzzy Control. Elsevier Science, U.S.A.
- [13] Şen Z (2001) Fuzzy Logic and Modeling Principles (Bulanık Mantık ve Modelleme Ilkeleri). Bilge Kültür Sanat Yayınevi, Istanbul (in Turkish).
- [14] Mellal A (2000) Derivation of seismic response spectra from the combination of fuzzy logic theory and a nonlinear numerical model. In:Proceedings of the 12 World Conference of Earthquake Engineering. Orléans, France.
- [15] Wadia-Fascetti S, Güneş B (2000) Earthquake response spectra models incorporating fuzzy logic with statistics. Computer-Aided Civil and Infrastructure Engineering 15(2):134-146.
- [16] Ansari A, Noorzad A (2004) A new method for calculation of fuzzy response spectra of earthquake motion in lowland. Lowland Technology International 6(1):21-32.
- [17] Marano GC, Morrone E, Sgobba S, Chakraborty S (2010) A fuzzy random approach of stochastic seismic response spectrum analysis. Engineering Structures 32(12):3879-3887.
- [18] Şen Z (2010) Rapid visual earthquake hazard evaluation of existing buildings by fuzzy logic modeling. Expert Systems with Applications 37(8):5653-5660.
- [19] Şen Z (2011) Supervised fuzzy logic modeling for building earthquake hazard assessment. Expert systems with applications 38(12):14564-14573.
- [20] Heidari PS, Khorasani M (2012) Generation of artificial earthquake accelerogram compatible with spectrum using the wavelet packet transform and nero-fuzzy networks. International Journal of Environmental, Chemical, Ecological, Geological and Geophysical Engineering 6(8):566-569.
- [21] Ozkul S, Ayoub A, Altunkaynak A (2014) Fuzzy logic based inelastic displacement ratios of degrading RC structures. Engineering Structures 75(4):590-603.
- [22] Bektaş N, Kegyes-Brassai O (2023) Development in fuzzy logic-based rapid visual screening method for seismic vulnerability assessment of buildings. Geosciences 13(1): 6.
- [23] Nahhas TM (2005) A fuzzy inference model for generating code-compliant seismic design response spectra. Umm Al-Qura University. J. Sci. Me. Eng 17(2):231-254.
- [24] Mangir A (2023) Fuzzy inference system (FIS) model for the seismic parameters of code-based earthquake response spectra. Buildings 13(8):1895.
- [25] Amirkhani A, Nasiriyan-Rad H, Papageorgiou EI (2020) A novel fuzzy inference approach: neuro-fuzzy cognitive map. International Journal of Fuzzy Systems 22(3):859-872.
- [26] Groumpos PP (2018) Intelligence and fuzzy cognitive maps: scientific issues, challenges, and opportunities. Studies in Informatics and Control 27(3):247-264.
- [27] Bakhtavar E, Valipour M, Yousefi S, Sadiq R, Hewage K (2021) Fuzzy cognitive maps in systems risk analysis: a comprehensive review. Complex & Intelligent Systems 7(4):621-637.
- [28] Al-Fahdawi OA, Barroso LR (2021) Adaptive neuro-fuzzy and simple adaptive control methods for full three-dimensional coupled buildings subjected to bi-directional seismic excitations. Engineering Structures 232:111798.
- [29] Ghani S, Kumari S, Ahmad S (2022) Prediction of the seismic effect on liquefaction behavior of fine-grained soils using artificial intelligence-based hybridized modeling. Arabian Journal for Science and Engineering 47(4):5411-5441.
- [30] Mehrabi P, Honarbari S, Rafiei S, Jahandari S, Alizadeh Bidgoli M (2021) Seismic response prediction of FRC rectangular columns using intelligent fuzzy-based hybrid metaheuristic techniques. Journal of Ambient Intelligence and Humanized Computing 12:10105-10123.
- [31] Tombari A, Stefanini L (2019) Hybrid fuzzy–stochastic 1D site response analysis accounting for soil uncertainties. Mechanical Systems and Signal Processing 132(1):102-121.
- [32] Guo M, Huang H, Xue C, Huang M (2022) Assessment of fuzzy global seismic vulnerability for RC structures. Journal of Building Engineering 57:104952.
- [33] AFAD (2022) Turkey Earthquake Regions Risk Map. Available at: afad.gov.tr/Türkiye-deprem-tehlike-haritasi
- [34] MATLAB (2023) version 9.14.0.2206163 (R2023a), Mathematical Computing Software for Engineers and Scientists, The MathWorks Inc., U.S.A.
- [35] Ross TJ (2016) Fuzzy Logic with Engineering Applications, Fourth Edition. John Wiley & Sons, USA.

[36] Oğuz U (2022) Comparison of Ground Motion Scaling Methods by Considering Vertical Ground Motions. MSc Dissertation, Middle East Technical University.

[37] Travasarou T, Bray JD, Abrahamson NA (2003) Empirical attenuation relationship for arias intensity. Earthquake Engineering & Structural Dynamics 32(7):1133-1155.